Local Perturbation in Bi_2CuO_4: Hydrothermal Synthesis, Crystal Structure, and Characterization of the New $Bi_2(Cu_{1-2x}M_x)O_4$ (M = Bi, Pb)

N. Henry, O. Mentre,* J. C. Boivin, and F. Abraham

Laboratoire de Cristallochimie et Physicochimie du Solide, UPRES A CNRS 8012, E.N.S.C.L., Université des Sciences et Technologies de Lille, BP 108, 59652 Villeneuve d'Ascq Cedex, France

Received June 21, 2000. Revised Manuscript Received November 20, 2000

Two new compounds $Bi_2(Cu_{1-2x}M_x)O_4$ (M = Bi, Pb) have been hydrothermally synthesized and structurally characterized. Hydrothermal treatment of $Bi_6O_5(NO_3)_5(OH)_3{\cdot}5H_2O$, $Pb(NO_3)_2$, and CuO mixtures in NaOH solution at 180 °C for a week yielded single crystals having the nonstoichiometric compositions $Bi_{2.08}Cu_{0.84}O_4$ and $Bi_2Pb_{0.04}Cu_{0.92}O_4$ depending on the starting mixture. The two compounds crystallize tetragonally, *P*4/*ncc*, $Z = 4$ with $a = 8.588(3)$ Å, $c = 5.799(2)$ Å and $a = 8.535(4)$ Å, $c = 5.812(3)$ Å for $Bi_{2.08}Cu_{0.84}O_4$ and $Bi_2Pb_{0.04}Cu_{0.92}O_4$, respectively. The structure refinements based on 157 and 155 independent reflections respectively converged to R1 = 0.036, wR2 = 0.069 and R1 = 0.049, wR2 = 0.121, respectively. The parent compound Bi_2CuO_4 structure consists of CuO_4 square-planar units stacked one on top of another in a staggered manner by Bi^{3+} ions along the *c* axis. The $(CuO_4)_8$ columns are connected by Bi^{3+} ions. In these new compounds, two consecutive Cu^{2+} ions are randomly removed and an M ion (M = Bi^{3+}, Pb^{2+}) occupies the site at the middle of the two copper vacancies and are thus 8-fold-coordinated by oxygen atoms. This involves the presence of a mixed $Cu^{2+/3+}$ valence state. Magnetic measurements indicated a low-temperature behavior different from that of the solid-state-prepared Bi_2CuO_4, but very similar to the Bi_2CuO_4 samples previously hydrothermally synthesized, which have the nonstoichiometric composition $Bi_2(Cu_{1-2x}Bi_x)O_4$ with an as yet undetected low *x* value. The present compounds are the first hydrothermally prepared Bi_2CuO_4-derived oxides whose structures have been fully determined.

Introduction

In connection with the high-T_c copper oxide problem, non-superconducting phases containing copper have attracted much interest. In that frame, the structural and magnetic properties of Bi_2CuO_4 have stimulated many studies in the past decade, notably because it represents an interesting example of a three-dimensional $S = {}^1/_2$ Heisenberg antiferromagnet, $T_N = 42$ K. It still attracts special attention in fundamental physics and is the object of numerous investigations using various techniques. For example, the phonon and magnon excitations in Bi_2CuO_4 were investigated using IR and Raman spectroscopy.[1,2] The inelastic neutron scattering experiments[3,4] as well as the antiferromagnetic resonance experiment (AFMR)[5−8] showed the three-dimensional character of the magnetic ordering. The spin waves were also analyzed using Raman[9] and neutron scattering experiments.[10,11] The anisotropy of the *g* factor of Cu^{2+} was also investigated because of the compound's interesting crystal structure.[12] In short, Bi_2CuO_4 is a huge field of study and one could wonder why it is still attractive for solid-state chemistry. Actually, this material has given rise to many controversies in numerous articles. It was initially discovered by Boivin et al as the only stoichiometric compound existing in the Bi_2O_3−CuO binary diagram.[13] It adopts a tetragonal symmetry, space group *P*4/*ncc*, but this first point was contested by Arpe and Muller-Buschbaum who assigned the *I*4 space group.[14] This last structural

* To whom correspondence should be addressed.

(1) Konstantinovic, M. J.; Konstantinovic, Z.; Popovic, Z. V. *Phys. Rev. B* **1996** , *54* (1), 68.
(2) Popovic, Z. V.; Kliche, G.; Konstantinovic, M. J.; Revcoleschi, A. *J. Phys. Condens. Matter* **1992**, *4*, 10085.
(3) Ong, E. W.; Kwei, G. H.; Robinson, R. A.; Ramakrishna, B. L.; von Dreele, R. B. *Phys. Rev. B* **1990**, *42*, 4255.
(4) Yamada, K.; Takada, K.; Hosaya, S.; Watanabe, Y.; Endoh, Y.; Tomonaga, N.; Suzuki, T.; Ishigaki, T.; Kamiyama, T.; Asano, H.; Izumi, F. *J. Phys. Soc. Jpn.* **1991**, *60* (7), 2406.
(5) Ohta, H.; Yoshida, K.; Matsuka, T.; Nanba, T.; Motokawa, M.; Yamada, K.; Endo, Y.; Hososya, S. *J. Phys. Soc. Jpn.* **1992**, *61* (8), 2921.
(6) Sviskov, L. E.; Chubarenko, V. A.; Ya. Shapiro, A.; Zalessky, A. V.; Petrakovskii, G. A. *J. Exp. Theor. Phys.* **1998**, *86* (6), 1228.
(7) Pankrats, A. I.; Sobyanin, D. Yu.; Vorotinov, A. M.; Petrakovskii, G. A. *Solid State Commun.* **1999**, *109* (4), 263.
(8) Ohta, H.; Ikeuchi, Y.; Kimura, S.; Okubo, S.; Nojiri, H.; Motokawa, M.; Hososya, S. K.; Yamada et Endo, Y. *Physica B* **1998**, *246−247*, 557.
(9) Konstantinovic, M. J.; Popovic, Z. V.; Devic, S. D.; Revcolevschi, A.; Dhalenne, G. *J. Phys.: Condens. Matter.* **1992**, *4*, 7913.
(10) Ain, M.; Dhalenne, G.; Guiselin, O.; Hennion, B. *Phys. Rev. B* **1993**, *47* (13), 8167.
(11) Roessli, B.; Fak, B.; Fernandez-Diaz, M.-T.; Sablina, K.; Petrakovskii, G. *Physica B* **1997**, *234−236*, 726.
(12) Tanaka, N.; Motizuki, K. *J. Phys. Soc. Jpn.* **1998**, *67* (5), 1755.
(13) Boivin, J. C.; Trehoux, J.; Thomas, D. *Bull. Soc. Fr. Minér. Cristallogr.* **1976**, *99*, 193.
(14) Arpe, R.; Muller-Buschbaum, H. K. *Zeits. Anorg. Allg. Chem.* **1976**, *426*, 1.

10.1021/cm000509t CCC: $20.00
Published on Web 01/19/2001

Table 1. Lattice Parameters (Å) for Bi_2CuO_4 Isotypic Coumpounds

compound	a	c
Bi_2CuO_4[17]	8.5039(1)	5.7999(1)
Bi_2PdO_4[24−26]	8.622(3)	5.907(3)
Bi_2AuO_5[15]	8.6703(4)	6.0301(3)
$Bi_4Au_2O_9$[15] (orthorhombic)	$a = 8.847(2)$ $b = 4 \times 8.668(2)$	$c = 5.889(1)$
$Bi_{2.08}Cu_{0.84}O_4$[a]	**8.588(3)**	**5.799(2)**
$Bi_2Pb_{0.04}Cu_{0.92}O_4$[a]	**8.535(4)**	**5.812(3)**
$(Bi_{2-x}Pb_x)PdO_4$[28] $(0 \le x \le 0.009)$	8.622(3)−8.642(1)	5.907(3) to ∼5.86
$(Bi_{2-x}Pb_x)PtO_4$[27−29] $(0.33 \le x \le 0.52)$	8.758(2)−8.769(2)	∼5.665 to ∼5.63
$Bi_{1.925}Pb_{0.075}Pd^{II}_{0.9625(1-x)}Cu^{II}_{0.9625x}Pd^{IV}_{0.0375}O_4$[29] $(0 \le x \le 1)$	∼8.65−8.50	∼5.87−5.82
$Bi_{1.57}Pb_{0.43}Pt^{II}_{0.785(1-x)}Cu^{II}_{0.785x}Pt^{IV}_{0.215}O_4$[29] $(0 \le x \le 1)$	∼8.75−8.57	∼5.65−5.80

[a] Present study.

hypothesis is now clearly refuted. From a magnetic point of view, Bi_2CuO_4 was initially inferred to be a one-dimensional antiferromagnet.[15] However, later neutron investigations[3−4,16−19] revealed undoubtedly a three-dimensional antiferromagnetic ordering as a ground state. Furthermore, some discrepancies were reported concerning the magnetic structure and notably the Cu^{2+} spin directions in the inorganic framework. Two types of magnetic structures were announced by several authors. The spins were first proposed to be directed along the [001] axis.[3,16−17] It is now admitted, since latter works,[4,10,18] that the spins are parallel to the (*a*,*b*) plane and align ferromagnetically along the [001] axis and antiferromagnetically between columns of stacked CuO_4 planes. This model was, for instance, confirmed by AFMR measurement.[5] We must therefore notice that, in a recent published paper, Konstantinovic et al. re-proposed the possibility of the *c*-axis orientation of the magnetic moments after a two-magnon light scattering in Bi_2CuO_4.[6] Finally, as an extra complication, it was observed that the static magnetic characteristics of samples depend sensitively on their preparative route. Effectively, several groups grew single crystals in hydrothermal conditions and observed a small spontaneous moment with an applied field perpendicular to [001]. At this level, a possible slight canting or an incomplete compensation of magnetic moments of two magnetic sublattices were involved despite the fact that no satisfying structural modification was noticed.[6,20−22] Our work partially answers this last point. It was initially motivated by the publication of a study concerning two novel ternary oxoaurates, $Bi_2Au^{3+}O_{4.5}$ and $Bi_2Au^{4+}O_5$ that adopt the Bi_2CuO_4 crystal structure and possess extra oxygen atoms in the framework.[23] It is noteworthy that several mixed valence oxides (Bi, $Pb)_2MO_4$ and (Bi, $Pb)_2$(Cu, M)O_4 with M = Pt, Pd were also prepared by solid-state reaction and studied.[24−29] Their formulas and lattice parameters are reported in Table 1. Thus, the potential to partially increase the copper oxidation number from +2 to +3 in this material led us to attempt synthesis in oxidizing conditions. This led to the preparation using hydrothermal techniques of two new compounds of the formula $Bi_2M_xCu_{1-2x}O_4$ with M = Bi ($x = 0.08$) and M = Pb ($x = 0.04$). They are mainly isostructural with Bi_2CuO_4 but present slight structural changes that modify their magnetic properties in a way similar to that already observed. The surprising behavior of previously studied hydrothermally prepared samples may be due to the same kind of defects in undetected amounts. This paper is devoted to the preparation, crystal structure, thermal behavior, and magnetic characterization of these two new phases.

Experimental Section

Synthesis of $Bi_{2.08}Cu_{0.84}O_4$ and $Bi_2Pb_{0.04}Cu_{0.92}O_4$. A number of samples were prepared using the following general conditions. The main procedure consists of an intimate grinding of precursors: bismuth nitrate, CuO in variable ratios. It is important to ensure that the bismuth precursor used is the so-called commercial basic nitrate bismuth of real formula $Bi_6O_5(NO_3)_5(OH)_3{\cdot}5H_2O$. Several attempts using $Bi(NO_3)_3{\cdot}5H_2O$ mainly yielded Bi_2CuO_4. About 1 g of the mixture was then placed in a 23-mL Teflon-lined stainless steel autoclave with 15 mL of NaOH solution and then heated at 180 °C for several days. The resulting product (powder or single crystals) was filtered, water washed, dried at room temperature, and then checked by X-rays using a D-5000 Siemens diffractometer. The first clues of the appearance of a new phase were given by the coexistence on X-ray diffraction patterns of the pure Bi_2CuO_4 phase accompanied by a "modified" Bi_2CuO_4-type phase (*mod*. Bi_2CuO_4) with slightly different parameters. Thus, several synthesis parameters were optimized to isolate the pure derivative compound. Various NaOH concentrations from 0.7 to 5 mol L^{-1} were tested. Optimal purity was obtained for $N = 2.2$ mol L^{-1} and this sample was retained for the study. Five days appears to be the optimal reaction time to obtain well-shaped single crystals. It is important to ensure that, despite our meticulous preparations, the reproducibility of the synthesis is not perfect and only few experiments led to the preparation of the pure *mod*. Bi_2CuO_4 that we used for the study. After an X-ray check, its purity was verified by density measurement, yielding 8.65(3) g cm^{-3} instead of the theoretical 8.61 g cm^{-3} value for the *mod*. Bi_2CuO_4. In the case of lead-substituted phases, $Pb(NO_3)_2$ was used as the precursor. In

(15) Sreedhar, K.; Ganguly, P.; Ramasesha, S. *J. Phys. C: Solid State Phys.* **1988**, *21*, 1129.
(16) Attfield, J. P. *J. Phys.: Condens. Matter* **1989**, *1*, 7045.
(17) Garcia-Munoz, J. L.; Rodriguez-Carjaval, J.; Sapina, F.; Sanchis, M. J.; Ibanez, R.; Beltran-Porter, D. *J. Phys.: Condens. Matter.* **1990**, *2*, 2205.
(18) Troc, R.; Janicki, J.; Filatow, I.; Fischer, P.; Murasik, A. *J. Phys.: Condens. Matter.* **1990**, *2*, 6989.
(19) Furrer, A.; Fischer, P.; Roessli, B.; Petrakovskii, G.; Sablina, K.; Valkov, V.; Fedoseev, B. *Solid State Commun.* **1992**, *82*, 443.
(20) Zalessky, A. V.; Krivenko, V. G.; Khimuch, T. A.; Ainbinde, N. E.; Bush, A. A. *J. Magn. Magn. Mater.* **1993**, *127*, 281.
(21) Szymczak, R.; Szymczak, H.; Zalessky, A. V.; Bush, A. A. *Phys. Rev. B* **1994**, *50* (5), 3404.
(22) Szymczak, R.; Szymczak, H.; Zalessky, A. V.; Bush, A. A. *J. Magn. Magn. Mater.* **1995**, *140−144*, 1573
(23) Geb, J.; Jansen, M. *J. Solid State Chem.* **1996**, *122*, 364.
(24) Boivin, J. C.; Conflant, P.; Thomas, D. *C. R. Acad. Sci. Paris* **1976**, *t282C*, 749.
(25) Arpe, R.; Muller-Buschbaum, H. K. *Z. Naturforsch* **1976**, *31b*, 1708.
(26) Conflant, P.; Boivin, J. C.; Thomas, D. *Rev. Chim. Miner.* **1977**, *t14*, 249.
(27) Boivin, J. C.; Conflant, P.; Thomas, D. *Mater. Res. Bull.* **1976**, *11*, 1503.
(28) Bettahar, N.; Conflant, P.; Boivin, J. C.; Abraham, F.; Thomas, D. *J. Phys. Chem. Solids* **1985**, *46* (3), 297.
(29) Bettahar, N.; Conflant, P.; Abraham, F. *J. Alloys Compd.* **1992**, *188*, 211.

Table 2. Crystal Data, Measurement, and Structure Refinement Parameters for $Bi_{2.08}Cu_{0.84}O_4$ and $Bi_2Pb_{0.04}Cu_{0.92}O_4$

	$Bi_{2.08}Cu_{0.84}O_4$	$Bi_2Pb_{0.04}Cu_{0.92}O_4$
	Crystal Data	
crystal symmetry	tetragonal	tetragonal
color	black	black
space group	*P*4/*ncc*	*P*4/*ncc*
cell dimension (Å)	$a = 8.580(5)$	$a = 8.535(4)$
	$c = 5.788(4)$	$c = 5.812(3)$
volume (Å)	425.5	423.4
Z	4	4
	Data Collection	
equipment	Bruker SMART CCD	Bruker SMART CCD
λ (Mo Kα (graphite monochromator)) (Å)	0.7107	0.7107
scan mode	ω	ω
θ range (deg)	3.33−23.14	3.38−23.08
recording reciprocal space	$-9 \le h \le 9$, $-7 \le k \le 9$, $-4 \le l \le 6$	$-8 \le h \le 9$, $-8 \le k \le 9$, $-6 \le l \le 6$
no. of measd reflns	1263	1592
no. of independent reflns	157	155
μ (mm^{-1}) (for λ Kα = 0.7107 Å)	89.8	85.76
limiting faces and distances (mm)	$1\bar{1}0$	empirical corrections
from an arbitrary origin	$\bar{1}\bar{1}0$ 0.0456	SADABS
	110	
	$1\bar{1}0$ 0.0456	
	001	
	$00\bar{1}$ 0.0129	
transmission factor range	0.006−0.107	
merging *R* factor	0.0564	0.0447
	Refinement	
no. of refined params	23	22
refinement method	least-squares on F^2	least-squares on F^2
R1(*F*)[$I > 2\sigma I$]/R1(*F*) [all data]	0.031/0.036	0.0392/0.0488
wR2(F^2) [$I > 2\sigma$I]/wR2(F^2) [all data]	0.067/0.069	0.114/0.121
$w = 1/(\sigma^2(F_o^2) + (0.0493P)^2 + 9.2976P)$ with $P = (F_o^2 + 2F_c^2)/3$		
GoF	1.383	1.185
extinction coefficient	0.0006(3)	
max/min $\Delta\rho$ Å e^{-3}	1.14/−1.21	3.78/−1.96

Table 3. Results of the Crystal Structure Refinements Considering Several Cations Nature in the M Site ($^1/_4$, $^1/_4$, *z*) (M = Na and O Models Are Clearly Rejected Since They Lead to Overfilled $(Cu_{Occ.Cu}/M_{Occ.M})O_4$ Columns

A	occupancy of M	occupancy of Cu	formula	*z*	U_{eq} (Å^2)[a]	R1	wR2
Bi	0.08(1)	0.84(2)	$Bi_{2.08}Cu_{0.84}O_4$	0.848(6)	0.039(9)	10.96	13.29
Na	0.51(1)	0.84(2)	$Bi_2Na_{0.51}Cu_{0.84}O_4$	0.846(6)	0.225(7)	10.96	14.19
O	0.95(1)	0.84(2)	$Bi_2Cu_{0.84}O_{4.95}$	0.850(6)	0.014(8)	10.98	14.14

[a] The U_{eq} values are defined by $U_{eq} = {}^1/_3(\sum_i\sum_j U_{ij}a_i^*a_j^*a_ia_j)$.

the same experimental conditions as above, it was not possible to prepare a single phase but only a mixture of three phases, Bi_2CuO_4, *mod*. Bi_2CuO_4, and *Pb-mod*. Bi_2CuO_4 using a Bi/Pb/Cu = 2/0.75/1 mixture of precursors. Single crystals of the third phase were present in the mixture.

Characterization. Density measurement was performed with an automated Micromeritics Accupyc 1330 helium pycnometer in a 1-cm^3 cell. Magnetic data were measured with a Quantum Design MPMS-XL5 SQUID magnetometer equipped with the ac susceptibility measurement M120-5S option. Susceptibility measurements were made in an applied field of 300 Oe and 1 kOe upon cooling from 295 to 2 K. ac susceptibility measurement was performed with a 3.5-Oe applied field at 20 Hz from 60 to 2 K. The hysteresis cycle was measured at 2 K between 50 and −50 kOe. The high-temperature X-ray diffraction diagrams were measured using a Guinier-Lenné diffraction system. For parameter refinement, a set of high-temperature data was also measured on a Siemens D-5000 powder diffractometer equipped with a Anton Paar HTK 1200 high-temperature oven camera from room temperature to 700 °C. GTA was performed with a TGA 92 SETARAM device.

X-ray Single-Crystal Structural Analysis. A black plate single crystal of *mod*. Bi_2CuO_4 was selected from a preparation containing only Bi and Cu precursors as explained above. Single-crystal X-ray diffraction intensities were measured on a Bruker SMART CCD detector diffractometer under the conditions shown in Table 2. The announced lattice parameters were refined from the complete data set (Table 2). An absorption correction using faces indexation was performed with the program XPREP of the SHELXTL block.[30] The pertinent data are summarized in Table 2. The program SHELXL was used for the refinement performed in the *P*4/*ncc* space group predicted by systematic extinctions. The Bi atom was located using the Patterson map while subsequent Fourier difference calculations located the Cu atoms yielding R1 = 0.108 and wR_2 = 0.486. At this point the Bi and Cu positions are similar to those observed in Bi_2CuO_4. Two intense peaks were then observed in the next Fourier difference map with heights 11.1 and 8.5 e Å^3. The most intense was located between two copper atoms and assigned to the partial substitution of a central M for two surrounding copper atoms. The results of the different refinements varying M (Bi, Na, O) are presented in Table 3. Only the Bi case satisfactorily matches the crystal structure since an independent refinement of Bi and Cu occupancies led to 0.08(1) and 0.84(2), respectively. This result is rather satisfying since "0.84 + (2 × 0.08) = 1" involves no vacancies along the Cu/Bi sequence. The other models would lead to overfilled Cu/M columns involving a Cu−O or Cu−Na distance of 1.3 Å. The second peak corresponds to the oxygen atom. In the last cycles of refinement anisotropic thermal parameters

(30) Sheldrick, G. M. *SHELXTL NT ver. 5.1*; Bruker Analytical X-ray Systems, Karlsruhe, Germany, 1998.
(31) Rodriguez-Carjaval, J. *FULLPROF 98*; Laboratoire Leon Brillouin (CEA-CNRS): France, 1998.

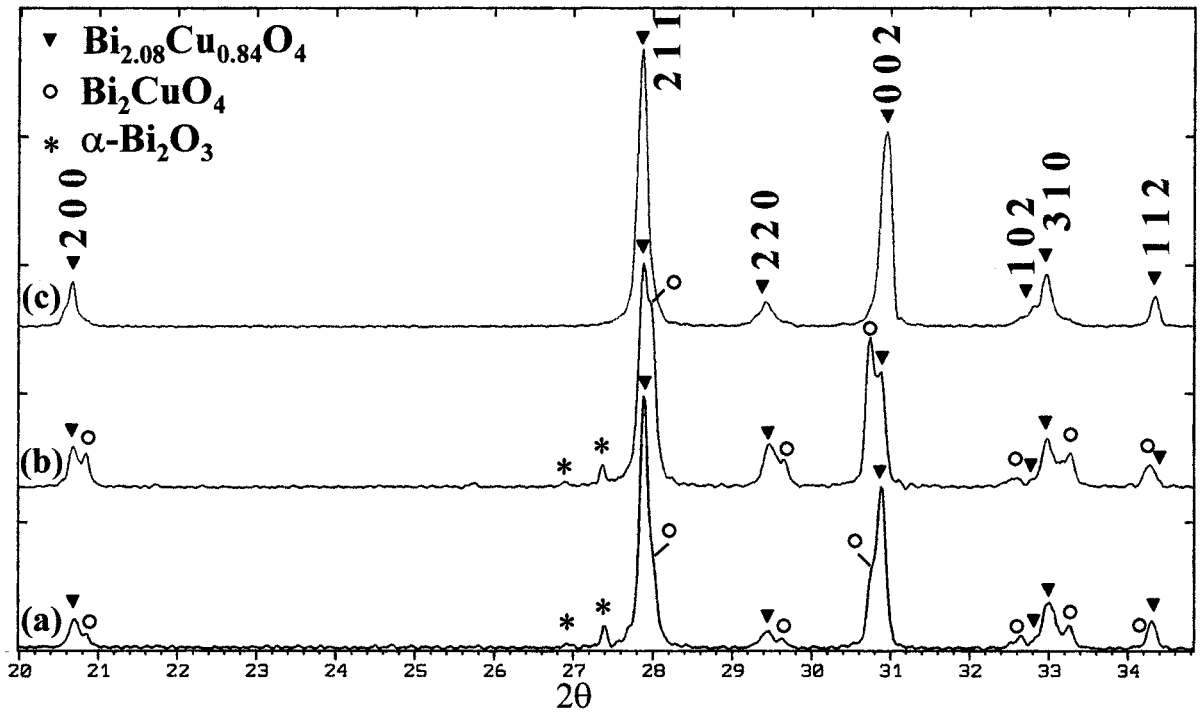

Figure 1. X-ray diffractograms of the prepared $Bi_{2.08}Cu_{0.84}O_4/Bi_2CuO_4$ mixture for various NaOH concentrations: (a) [NaOH] = 1.5 N/7 days, (b) [NaOH] = 3.7 N/7 days, and (c) pure compound; [NaOH] = 2.2 N/5 days.

Table 4. Positional Parameters and Anisotropic Displacement Parameters Factors for $Bi_{2.08}Cu_{0.84}O_4$ and *$Bi_2Pb_{0.04}Cu_{0.92}O_4$*

Positional Parameters

atom	site	occupancy factor	*x*	*y*	*z*	U_{eq} (Å^2)[a]
Bi(1)	8f	1	0.9190(1)	−0.9190(1)	0.25	0.013(1)
Bi	*8f*	*1*	*0.9177(1)*	*−0.9177(1)*	*0.25*	*0.019(1)*
Bi(2)	4c	0.08(1)	0.25	0.25	0.854(6)	0.05(1)[b]
Pb	*4c*	*0.04(1)*	*0.25*	*0.25*	*0.903(7)*	*0.01(2)*[b]
Cu	4c	0.84(2)	0.25	0.25	0.079(2)	0.009(2)
Cu	*4c*	*0.92(2)*	*0.25*	*0.25*	*0.075(1)*	*0.017(2)*
O	16g	1	0.550(2)	0.642(2)	0.409(3)	0.015(3)
O	*16g*	*1*	*0.548(2)*	*0.644(2)*	*0.407(3)*	*0.022(3)*

Anisotropic Temperature Coefficients (Å^2)[c]

atom	U_{11}	U_{22}	U_{33}	U_{12}	U_{13}	U_{23}
Bi(1)	0.014(1)	U_{11}	0.013(1)	0.004(1)	0.001(1)	U_{13}
Bi	*0.020(1)*	*U_{11}*	*0.017(1)*	*0.003(1)*	*0.001(1)*	*U_{13}*
Bi(2)	0.01(1)	U_{11}	0.21(7)	0	0	0
Cu	0.010(3)	U_{11}	0.006(3)	0	0	0
Cu	*0.015(2)*	*U_{11}*	*0.022(4)*	*0*	*0*	*0*
O	0.015(8)	0.011(8)	0.019(7)	0.001(7)	0.009(8)	0.004(7)
O	*0.015(6)*	*0.027(8)*	*0.025(7)*	*−0.006(6)*	*−0.002(7)*	*−0.003(8)*

[a] The U_{eq} values are defined by $U_{eq} = {}^1/_3(\sum_i\sum_j U_{ij}a_i^*a_j^*a_ia_j)$. [b] Atomic displacement type U_{iso}. [c] The anisotropic temperature is defined by $U = \exp[-2\pi^2(h^2a^{*2}U_{11} + k^2b^{*2}U_{22} + l^2c^{*2}U_{33} + 2hka^*b^*U_{12} + 2hla^*c^*U_{13} + 2klb^*c^*U_{23})]$.

were included as well as secondary extinction and an optimized weighting scheme, yielding the final R1 = 0.036 and wR2 = 0.069. Table 4 lists the atomic coordinates and displacement parameters. The unit formula deduced from the structure refinement is $Bi_{2.08}Cu_{0.84}O_4$.

Neutron Powder Rietveld Analysis. To check the potentially deficient oxygen stoichiometry, it was interesting to collect a neutron diffraction data set. In that frame, we benefited from extra neutron exposure time to measure the 2°−160° diffraction pattern, with a 0.05° 2θ step on a 2.5 g $Bi_{2.08}CuO_4/Bi_2CuO_4$ mixture. The D2B high-resolution diffractometer of the ILL, France, was used with $\lambda = 1.5939$ Å with a total exposure time of 4 h. Both phases were simultaneously refined using Fullprof 98,[32] yielding the final $\chi^2 = 1.515$, $R_p = 0.180$, and $R_{wp} = 0.175$: $Bi_{2.08}Cu_{0.84}O_4$, $R_f = 0.078$ and $R_{Bragg} = 0.0658$; Bi_2CuO_4, $R_f = 0.080$ and $R_{Bragg} = 0.0672$. The calculated, observed, and difference diffraction profile are presented in Figure 1, indicating a good match between the experimental and calculated patterns. The inset figure shows the strong overlapping of the peaks of the two phases because of their close relation. Nevertheless, the good convergence of the lattice parameters of each phase to their expected values makes the results reliable. As a matter of fact, the high background value is due to the relatively short exposure time. Two important features are to be noticed: (1) It was not possible to refine the occupancy and thermal factor for Bi(2) but its introduction with the fixed values deduced from the single-crystal study slightly lowered the reliability factors. (2) The refinement of the oxygen occupancy yields 1.022(15), in good agreement with a complete oxygen presence.

(32) *SAINT ver. 6.2*; Bruker Analytical X-ray Systems, Karlsruhe, Germany, 1999.

Table 5. Bond Lenghts (Å) and Angles (deg) for $Bi_{2.08}Cu_{0.84}O_4$, *$Bi_2Pb_{0.04}Cu_{0.92}O_4$*, and Bi_2CuO_4[a]

			Environment of Bi(1)				
$Bi(1)-O^{i/ii}$ (2×)	2.14(2)	*2.16(2)*	**2.133(1)**	$O^{i}-Bi(1)-O^{iii}$ (2×)	87.7(5)	*87.9(4)*	**88.28(5)**
$Bi(1)-O^{iii/iv}$ (2×)	2.33(2)	*2.35(2)*	**2.337(1)**	$O^{i}-Bi(1)-O^{iv}$ (2×)	77.1(6)	*77.3(6)*	**76.69(4)**
$Bi(1)-O^{v/vi}$ (2×)	2.79(2)	*2.74(2)*	**2.759(1)**	$O^{i}-Bi(1)-O^{ii}$	88.0(8)	*86.4(7)*	**87.82(5)**
$\sum_{ij} s_{ij}$ Bi(1)	3.12	*3.02*	**3.17**				
$Bi(1)-Bi(1)^{vii}$	3.496(1)	*3.520(2)*		Bi(1)−M	3.248(6)	*3.30(1)*	
Bi(1)−Cu	3.341(4)	*3.335(2)*					
Bi(1)−Lp			**0.634**				
			Environment of M with M = Bi or *M = Pb*				
				$O^{ix}-M-O^{iv}$ (4×)	68(2)	*62.5(8)*	
$M-O^{iv/vii/viii/ix}$(4×)	2.47(3)	*2.65(3)*		$O^{ix}-M-O^{iii}$ (4×)	100(2)	*94(2)*	
$M-O^{ii/v/x/xi}$ (4×)	2.38(2)	*2.24(2)*		$O^{x}-M-O^{v}$ (4×)	70(2)	*75.8(8)*	
$\sum_{ij} s_{ij}$ M	$3.28Bi^{3+}$	*$3.76Pb^{2+}$*		$O^{x}-M-O^{ii}$ (4×)	114(2)	*121(2)*	
M−Cu	4.19(4)	*3.91(5)*					
$M-Cu^{xii}$	4.48(4)	*4.81(5)*					
			Environment of Cu				
$Cu-O^{ii/v/x/xi}$ (4×)	1.95(2)	*1.95(2)*	**1.9348(9)**	$O^{x}-Cu-O^{v}$ (4×)	89.92(4)	*89.84(5)*	**89.89(3)**
$\sum_{ij} s_{ij}$ Cu	1.92	*1.92*	**2.00**	$O^{x}-Cu-O^{ii}$ (4×)	176(2)	*174(1)*	**175.0(1)**
$Cu-Cu^{xii}$	2.889(1)	*2.906(2)*	**2.910(3)**				

[a] (i) $^1/_2 - x$, $^1/_2 - y$, z; (ii) $^1/_2 + y$, $^1/_2 + x$, $^1/_2 - z$; (iii) $^1/_2 - y$, $^1/_2 - x$, $^1/_2 + z$; (iv) $^1/_2 + x$, $^1/_2 + y$, $\bar{z}$; (v) $^1/_2 + x$, $\bar{y}$, $^1/_2 - z$; (vi) y, $^1/_2 - x$, z; (vii) $\bar{x}$, $\bar{y}$, $\bar{z}$; (viii) $^1/_2 + y$, $\bar{x}$, $\bar{z}$; (ix) $\bar{y}$, $^1/_2 + x$, $\bar{z}$; (x) $\bar{y}$, $\bar{x}$, $^1/_2 - z$; (xi) $\bar{x}$, $^1/_2 + y$, $^1/_2 - z$; (xii) y, x, $^1/_2 + z$.

A single crystal of the third phase in the lead-containing mixture as described above was selected. In that case, because of the complexity of the shape, semiempirical absorption corrections were performed using the SADABS program.[33] Data collection and refinement data are given in Table 2. Initially, a Patterson calculation and subsequent Fourier difference syntheses yielded a structural model comparable to that of $Bi_{2.08}Cu_{0.84}O_4$, but the additional extra atom was assigned to Pb because of a different off-centering from the oxygen environment compared to that of the previous case. The occupancies related by the equation $Occ_{Cu} = 1-2Occ_{Pb}$ were refined to 0.04(1) and 0.92(2) for Pb and Cu, respectively. Final *R* factors including anisotropic atomic displacement parameters for Bi, Cu, and O atoms and an optimized weighting scheme are $R1 = 0.049$ and $wR_2 = 0.121$. The crystal was then removed from its glass fiber and a semiquantitative analysis was performed on a JEOL 5300 scanning electron microscope equipped with a PGT energy-dispersive spectrometer (EDS) using a germanium detection and an ultrathin window. It indicates a Pb/Bi ratio of 0.17/2, at least confirming the presence of Pb in the crystal. The unit formula deduced from the single-crystal structure refinement is $Bi_2Pb_{0.04}Cu_{0.92}O_4$.

Results and Discussion

Structure Description. Figure 2 presents the X-ray powder patterns obtained in different conditions showing different Bi_2CuO_4/*mod.* Bi_2CuO_4 ratios. Pure *mod.* Bi_2CuO_4 is presented at the top of the figure. All the observed lines of the powder pattern were indexed using the program TREOR.[33] The tetragonal lattice constants least-squares refined to $a = 8.588(3)$ Å, $c = 5.799(2)$ Å, $F(20) = 34$ (0.0169, 35) indicate the close structural relation with Bi_2CuO_4, $a = 8.5039(1)$ Å and $c = 5.8202(1)$ Å.[17] It is noteworthy that these phases show strong preferential orientation, explained by the strong change of the 002 intensity of the modified phase relative to that of the parent phase. The Bi_2CuO_4 crystal structure[13] is formed of isolated CuO_4 square-planar units of Cu^{2+} ions stacked one on top of another in a staggered manner to form columns along the *c* axis. The bismuth atoms are connected to CuO_4 planes through the $(BiO_2)_n$ chains parallel to *c*. In both new compounds, two consecutive copper atoms are randomly removed and a M cation (M = Bi, Pb) occupies the site between the two vacancies (Figure 3). Thus, M intervenes as a local perturbation cutting the infinite CuO_4 columns into isolated sections. Selected bond distances and angles are given in Table 5 for the two title compounds and for Bi_2CuO_4.[17] For both substituted compounds interatomic distances remain essentially unchanged as compared to those of Bi_2CuO_4. Only a slight increase of Cu−O distances due to the *a* lattice parameter dilatation is therefore observable. The interplay among lone-pair electrons (E) and crystal structure has long been of interest to crystallographers and solid-state chemists. The theory enabling the calculation for localizing the lone-pair electrons in a crystal structure was developed by Verbaere et al.[34] and was incorporated in the computer program HYBRIDE. The polarizability for Bi^{3+} was chosen as $\alpha = 6.12$ Å^3.[35] After an ionic model and a partial charge model for the atom was considered, satisfactory, self-consistent, lone-pair electron positions were obtained by the latter. The mean ionicity for each M chemical species was calculated for Bi_2CuO_4 from the electronegativity differences of the terminal atoms of the M−O bonds. Thus, a percentage formal ionicity value was calculated for each bond and applied to the oxidation state of the cation. This procedure yields +1.71 for Bi^{3+} and +1.07 for Cu^{2+}. The different oxygen atoms were given the balancing charge −1.12 to ensure electroneutrality within the lattice. The program HYBRIDE splits the polarizable Bi^{3+} into a mobile −2 charge for the E and a stationary +3 charge for the nucleus and the core orbitals. This calculation was performed for Bi_2CuO_4 crystal data and is assumed to be applicable to the Bi(1) of the two new $Bi_2(Cu_{1-2x}M_x)O_4$ (M = Bi, Pb) phases. Self-consistent E coordinates were found at $x = 0.866$, $y = -x$, and $z = ^1/_4$, leading to a Bi−E distance of 0.63 Å. Thus, *E* is, as commonly observed, located at the top of an E O4 Bi centered square pyramid. Lone pairs are 2 × 2, pointing toward

(33) Werner, P. E.; Eriksson, L.; Westdahl, M. *J. Appl. Crystallogr.* **1985**, *18*, 367.

(34) Verbaere, A.; Marchand, R.; Tournoux, M. *J. Solid State Chem.* **1978**, *23*, 383.

(35) Shannon, R. D. *Acta Crystallogr.* **1976**, *A32*, 751.

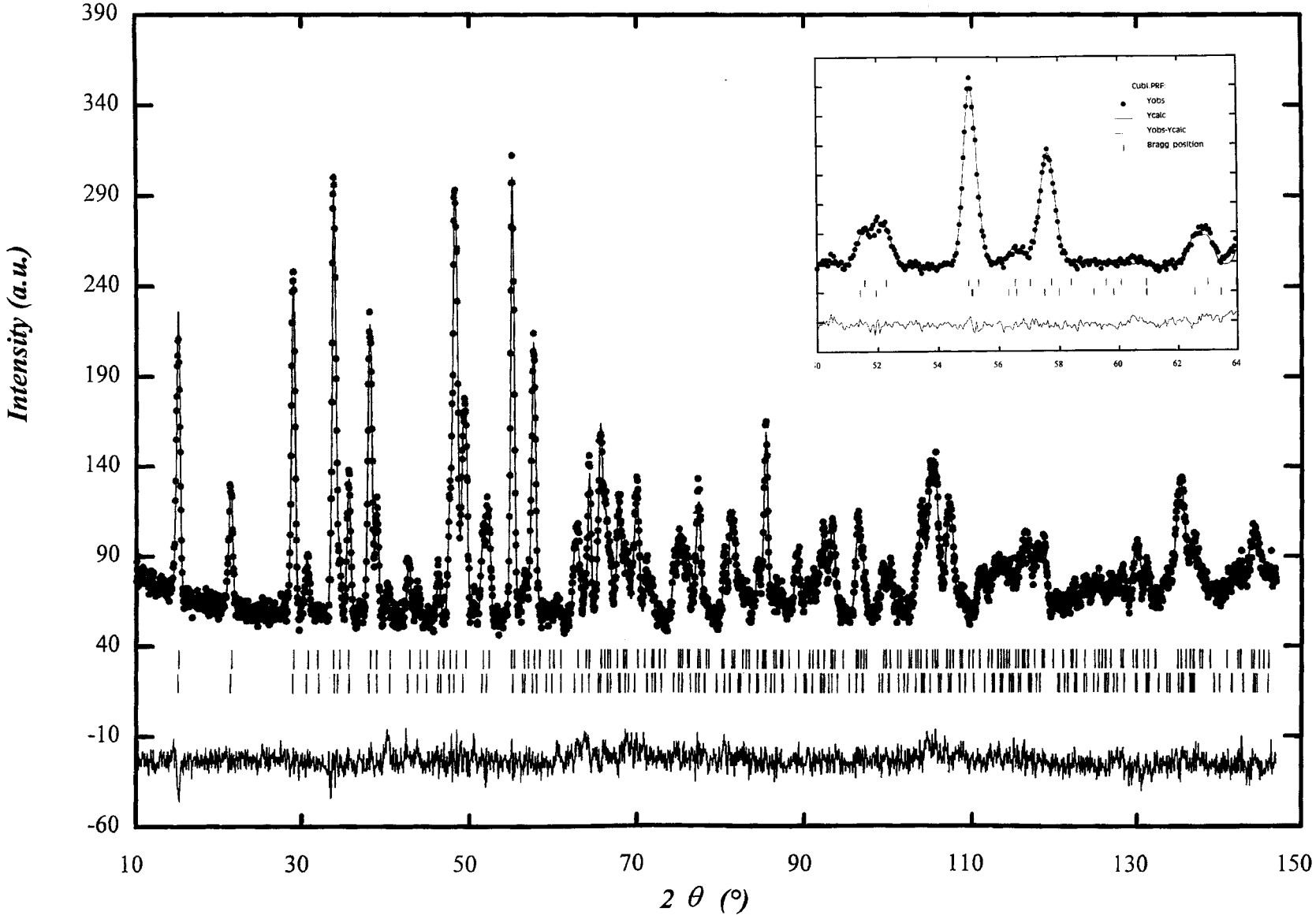

Figure 2. Calculated (lines), observed (dots), and difference diffraction profiles from neutron data at 290 K for a mixture of $Bi_{2.08}Cu_{0.84}O_4$ and Bi_2CuO_4.

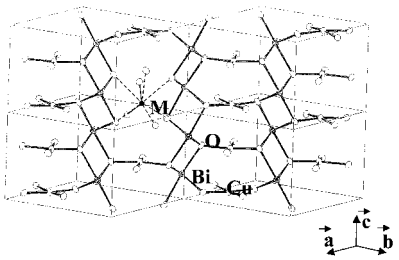

Figure 3. Structure of $Bi_2(Cu_{1-2x}M_x)O_4$ (only the atoms near the (110) plane are represented).

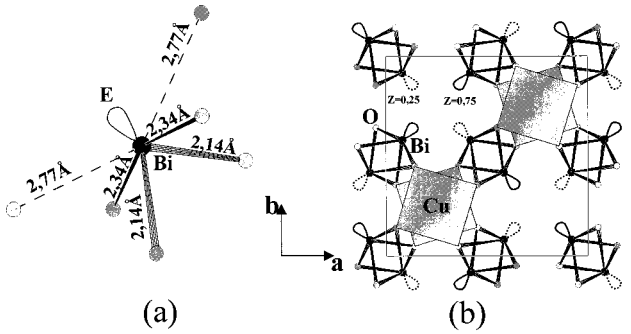

Figure 4. (a) Oxygen atom environment around Bi in Bi_2CuO_4. *E* stands for lone pair electrons. (b) Bi_2CuO_4 projection along the *c* axis.

the center of the empty space at $z = {}^1/_4$ and $z = {}^3/_4$ (Figure 4). In Bi_2AuO_5 , the extra oxygen atom is located in these interstices at $z = 0$ and $^1/_2$, which appear to be, from our calculations, a OBi_4 tetrahedral position (Bi−O = 2.455(1) Å).

Cationic Valence. In the case of $Bi_{2.08}Cu_{0.84}O_4$, M is surrounded by four bonded oxygens with Bi−O = 2.37(3) Å and four bonded oxygens with Bi−O = 2.54(3) Å, which form a O_8 antiprism. The off-centering is characteristic of a trivalent state because the $6s^2$ lone pair is stereoactive. A bond valence sum calculation using Bi^{3+} data from Brown and Altermatt[36] matches rather well, yielding +3.28. The refined stoichiometry involved a mixed +2/+3 valence for copper with an expected +2.09 mean charge. For $Bi_2Pb_{0.04}Cu_{0.92}O_4$, the M off-centering is greater than that for M = Bi with four 2.23(2) Å and four 2.65(3) Å M−O distances, involving a different cation. The bond valence sum using Pb^{2+}, Pb^{4+}, and Bi^{3+} yields the unsatisfactory +3.72, +3.08, and +3.56 valence units, respectively. These poor bond valence sums around M are not surprising. Since M is present in only a small fraction of the sites, the relaxed O positions will not contribute much to the refined O positions. Therefore, the EDS results combined with the M off-centering change from $Bi_{2.08}Cu_{0.84}O_4$ favor Pb^{2+} as a substituent. Since no significant replacement of Bi(1) by lead was achieved in Bi_2CuO_4,[28] we assume Bi^{3+}-only and Pb^{2+}-only occupancies for Bi(1) and M sites, respectively. The mean copper valence deduced from the refined stoichiometry is +2.08. As a matter of fact, for both compounds the same copper valence was reached in our oxidizing (H_2O pressure + NaOH) synthesis conditions. From a spectroscopic point of view, Cu^{2+} and Cu^{3+} are hardly distinguishable because of the low stability of the latter combined, in the case of superconducting cuprates to the presence of extra holes

(36) Brown, I. D.; Altermatt, D. *Acta Crystallogr.* **1985**, *B41*, 244.

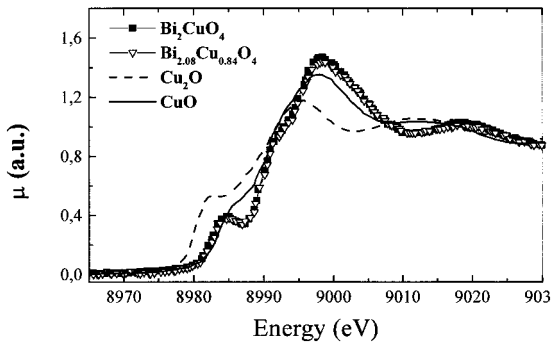

Figure 5. XANES spectra performed at the Cu K edge for Bi_2CuO_4, pure $Bi_{2.08}Cu_{0.84}O_4$, Cu_2O, and CuO.

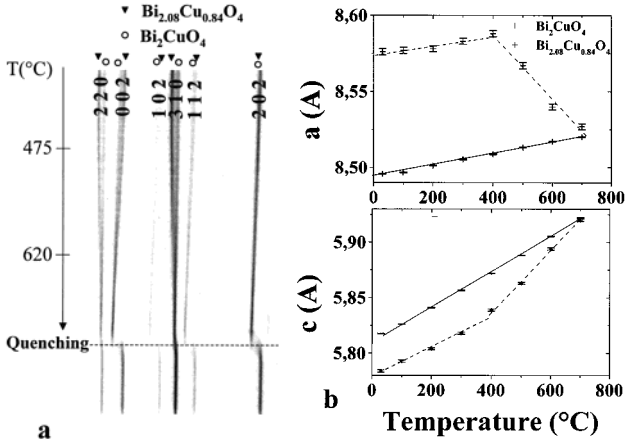

Figure 6. (a) High-temperature XRD characterization of a $Bi_2CuO_4/Bi_{2.08}Cu_{0.84}O_4$ mixture evidencing the transformation of the latter. (b)Comparison of the lattice parameters thermal evolution of Bi_2CuO_4 and $Bi_{2.08}Cu_{0.84}O_4$.

localized in the 2p oxygen valence band. Therefore, to distinguish between Cu^{2+} and possibly present Cu^+ cations (if oxygen vacancies exist), a XANES experiment was performed at the Cu−K edge for Bi_2CuO_4 and pure $Bi_{2.08}Cu_{0.84}O_4$ using the D21 spectrometer at DCI, Lure synchrotron radiation facility. The obtained spectra are given in Figure 5 and compared to CuO and Cu_2O spectra taken in the same conditions. For the two Bi−Cu−O compounds, the edges are similar and characteristic of a square planar coordination. The peaks at 8985 and 8998 eV are assigned to the 1s → 4pz* and 4p*x*,*y**, respectively. The shoulder at 8991 eV is a shakedown of the latter; that is, a 2p ligand electron transits to a vacant copper 3d state. As observed, the spectra are very similar to the CuO spectrum while no Cu^+ component is observed. These results at least exclude the possibility of copper-reduced species.

Thermal Behavior of $Bi_{2.08}Cu_{0.84}O_4$. A preliminary high-temperature XRD characterization of a $Bi_2CuO_4/Bi_{2.08}Cu_{0.84}O_4$ mixture is presented in Figure 6a. The peaks of the latter start to deviate toward that of the former at about 400 °C. At 620 °C only Bi_2CuO_4 remains in the pattern. Additional Bi_2O_3 within the mixture was not observed with the Guinier-Lenné camera but was evidenced on the D5000 diffractograms. So the substituted phase progressively decomposes into a Bi_2CuO_4 and Bi_2O_3 mixture. This feature is clearly observed in Figure 6b, which shows the comparison of the lattice parameter's thermal evolution of two pure samples. Bi_2CuO_4 lattice parameters linearly increase versus the

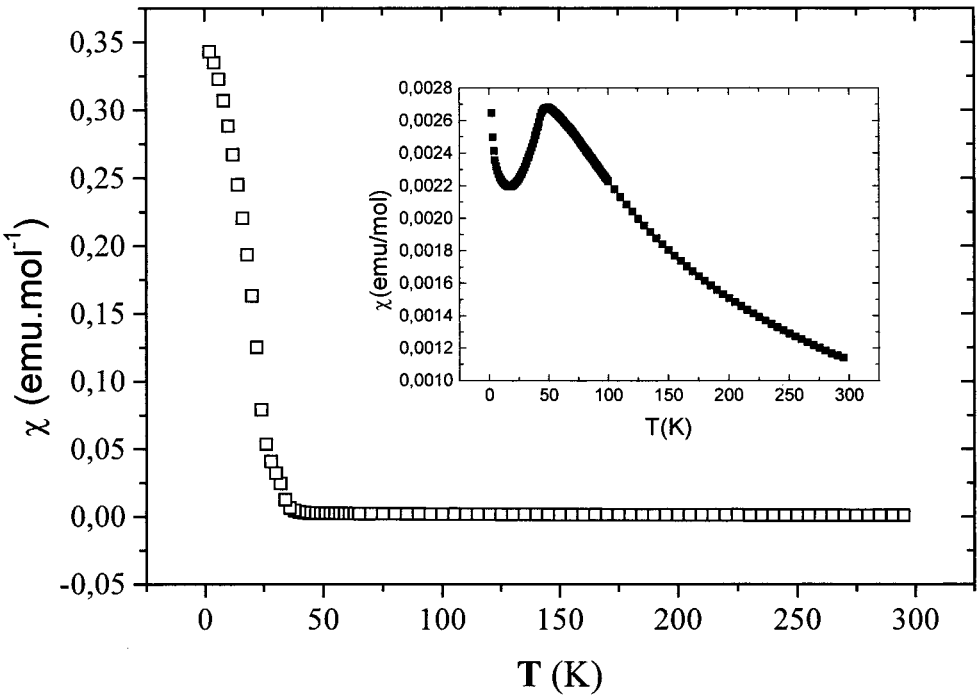

Figure 7. Magnetic susceptibility versus temperature measured for hydrothermally prepared $Bi_{2.08}Cu_{0.84}O_4$. The solid-state-prepared Bi_2CuO_4 plot is shown in the inset (with different χ scales for both figures).

temperature in the same way as $Bi_{2.08}Cu_{0.84}O_4$ from room temperature to 400 °C. At that point a strong break is observed, corresponding to the structural reorganization of $Bi_{2.08}Cu_{0.84}O_4$ completed at 700 °C. The 400−700 °C range corresponds to the presence of intermediate $Bi_{2+x}Cu_{1-2x}O_4$ with $x \leq 0.08$ corresponding to a 2.09−2 copper valence range. At this point, it is noteworthy that even if intermediate materials exist, our synthesis conditions only lead to a modified phase with a copper valence close to 2.09.

The calculated weight loss associated with the reduction of one $Bi_{2.08}Cu_{0.84}O_4$ to 0.84 Bi_2CuO_4 and 0.2 Bi_2O_3 is 0.115%, an undetectable value. As expected, a flat line was observed during the TG analysis.

Magnetic Properties. Figure 7 shows the magnetic susceptibility versus temperature measured for hydrothermally prepared $Bi_{2.08}Cu_{0.84}O_4$ and Bi_2CuO_4 prepared by solid-state reaction in the inset. As discussed in the Introduction, the latter was intensively studied for the three-dimensional nature of its antiferromagnetism. The paramagnetic domain occurring above $T_N \approx 40$ K was modeled by a Curie−Weiss law $\chi^{-1} = (T - \theta_c)/C$ with $\theta_c = -98.8$ K and $C = 0.45$ emu K mol^{-1}. The deduced value $\mu_{eff} = 1.89\ \mu_B$/Cu is in good accordance with previous works.[15,18] It is slightly higher than the expected value of 1.73 μ_B for a Cu^{2+} spin only contribution because of a large spin−orbit coupling causing a g value of 2.18 instead of 2. The sudden increase of χ below 2 K is due to parasitic paramagnetism due to magnetic impurities. As a matter of fact, $Bi_{2.08}Cu_{0.84}O_4$ magnetic behavior drastically differs. A spontaneous magnetic moment appears below 40 K involving a weak ferromagnetism induced by the CuO_4 infinite columns cutting in sections. In the paramagnetic state a Curie−Weiss law was fitted, yielding $\theta_c = -91.2$ K and $C = 0.34$ emu K mol^{-1}. This value corresponds to an effective moment $\mu_{eff} = 1.65\ \mu_B$/FU. Considering 0.76 paramagnetic Cu^{2+} (d,[9] $S = 1/2$) and 0.08 diamagnetic Cu^{3+} (d,[8]

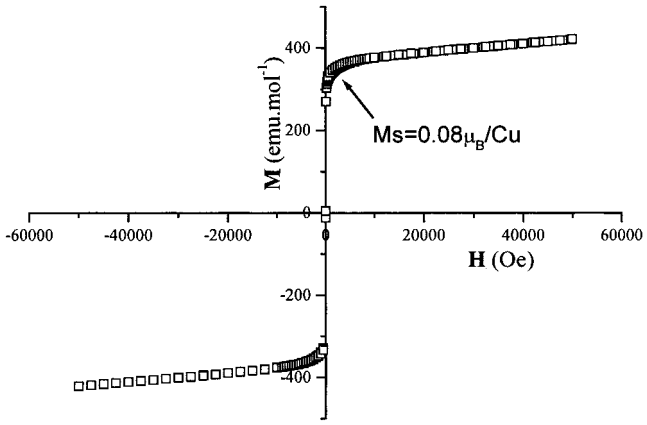

Figure 8. M vs H hysteresis cycle at 2 K for $Bi_{2.08}Cu_{0.84}O_4$.

$S = 0$) per formula unit, we obtain the identical $\mu_{eff} = 1.89\ \mu B/Cu^{2+}$ value in good agreement with the mixed valence character reported above. The magnetization versus H hysteresis curve from −50 to 50 KOe at 2 K shows no coercitive effect (Figure 8). Saturation is obtained for a very low applied field. The saturation value at $H = 0$ extrapolated from the linear part of the M vs H plot corresponds to 0.067 μB/FU or 0.088 $\mu B/Cu^{2+}$. The spontaneous inversion of the magnetization upon H reversal is also evidenced by the nearly null value of the M'' imaginary part of the ac susceptibility measured at 20 Hz, $H = 3.5$ Oe (Figure 9). The resulting magnetization $M = \sqrt{(M'^2+M''^2)}$ is superimposable to its real part M'.

Several previous works performed on hydrothermally grown Bi_2CuO_4 single crystals have revealed in the ordered state a small ferromagnetic moment m in the basal plane of <1% of the nominal Cu^{2+} magnetic moment.[6,20−22] This value is therefore lower than the 8.8% estimated above for $Bi_{2.08}Cu_{0.84}O_4$. It was also observed that the weak ferromagnetism drops as the

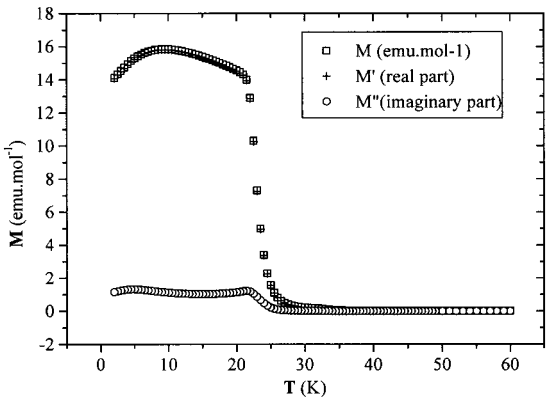

Figure 9. ac susceptibility data measured at 20 Hz, H = 3.5Oe.

static field increases and vanishes for H > 30 KOe while, in our case, it still remains up to 50 KOe. Its origin was not clearly established and was proposed to occur either due to a slight Dzyaloskinski−Moria canting of Cu moments or due to the incomplete compensation of magnetic moments of two magnetic sublattices (domain walls). No structural distinction between hydrothermally and solid-state manufactured samples was observed, even if the authors did not exclude a possible orthorhombic distortion in the former. Actually, because of the similar methods of preparation, it is very tempting to assume that the studied crystals show the same kind of local perturbations as observed in this work but in undetectable amounts. Thus, in terms of perturbation, the two new $Bi_2(Cu_{1-2x}M_x)O_4$ compounds would represent extreme cases because of their preparation in a highly oxidizing medium. This justifies the 1 order of magnitude larger value of m measured from polycrystalline $Bi_{2.08}Cu_{0.84}O_4$. The observed elimination of the weak ferromagnetism after annealing in an oxygen or helium atmosphere[6] also supports our hypothesis since it was shown here that the distorted phases are transformed into Bi_2CuO_4 upon heating. Considering the disordered state of (Bi,Pb)-inclusions within CuO_4 columns, it seems probable that the origin of the spontaneous magnetization is related to magnetically uncompensated antiferromagnetic domains magnetically isolated by the M sites.

Acknowledgment. We sincerely acknowledge Pr. M. Drillon and Dr. P. Rabu, IPCMS, CNRS UMR 7504, Strasbourg, France for the magnetic measurements. We are grateful to Dr. C. Godart and Dr. E. Alleno, LCMTR, CNRS UPR 209, Thiais, France, for the XANES experiments and for detailed discussions. Finally, we acknowledge N. Djelal and L. Burylo, LCPS, CNRS UPRES A 8012, Villeneuve d'Ascq, France, for the X-ray and thermal analysis experiments.

CM000509T